Nonunitary Operations for Ground-State Calculations in Near-Term Quantum Computers

Guglielmo Mazzola,[1,*] Pauline J. Ollitrault,[1,2] Panagiotis Kl. Barkoutsos,[1] and Ivano Tavernelli[1]
[1]IBM Research Zurich, Säumerstrasse 4, 8803 Rüschlikon, Switzerland
[2]Laboratory of Physical Chemistry, ETH Zürich, 8093 Zürich, Switzerland

(Received 9 July 2019; published 27 September 2019)

We introduce a quantum Monte Carlo inspired reweighting scheme to accurately compute energies from optimally short quantum circuits. This effectively hybrid quantum-classical approach features both entanglement provided by a short quantum circuit, and the presence of an effective nonunitary operator at the same time. The functional form of this projector is borrowed from classical computation and is able to filter out high-energy components generated by a suboptimal variational quantum heuristic *Ansatz*. The accuracy of this approach is demonstrated numerically in finding energies of entangled ground states of many-body lattice models. We demonstrate a practical implementation on IBM quantum hardware up to an 8-qubit circuit.

DOI: 10.1103/PhysRevLett.123.130501

Solving quantum many-body and electronic structure problems is one of the most anticipated applications of quantum computers, in view of the exponential speed-up that can be achieved compared to classical simulations [1–3]. Despite decades of efforts, an efficient classical way to describe many-body effects and strong correlations is still missing, preventing classical computation of fermionic systems from reaching the desired accuracy in large-scale applications [4,5]. On the other hand, quantum computation is still at its infancy and state-of-the-art calculations are performed on so-called noisy intermediate quantum (NISQ) hardware, of 20–50 qubits [6].

These nonideal conditions, represented by short circuit depths and the absence of implementable error correction schemes, call for the development of suitable algorithms able to exploit the present resources [7,8]. In this context, variational approaches have been proposed as near-term strategy to solve the electronic structure problem [9–12]. These algorithms drastically reduce the coherence time requirement, but feature optimizable parameters $\boldsymbol{\theta}$ in the circuit, generating a parametrized quantum state $|\psi_c(\boldsymbol{\theta})\rangle$. These parameters are optimized to minimize the energy $\langle\psi_c(\boldsymbol{\theta})|\mathcal{H}|\psi_c(\boldsymbol{\theta})\rangle$ for a given problem Hamiltonian $\mathcal{H}$. The energy is calculated as a sum of expectation values of Pauli operators; hence, the circuit is executed multiple times to reduce the variance of such estimates. The parameter optimization is instead performed classically [9]. This approach, called variational quantum eigensolver (VQE), has been applied to small molecules and quantum magnets [13–16], and relies on the assumption that a quantum state prepared in a quantum computer can represent efficiently and compactly all the correlations that are hard to encode classically [17].

Lattice many-body models represent an ideal test bed for developing new algorithms, since they retain all the features that make electronic structure problems hard to simulate classically, but without the specific overcomplication of quantum chemistry [18].

A concrete example is the Hubbard model, which is perhaps the most extensively studied condensed matter system, as it serves as a minimal model for high-temperature superconductors [19] and other correlation-driven phase transitions [20]. Polynomially scaling classical algorithms can obtain accurate solution only under particularly symmetric conditions such as two-dimensional (2D) lattices at half-filling [5].

The most advanced classical algorithms, such as quantum Monte Carlo (QMC) calculations or density matrix renormalization group theory [21] are also characterized by underlying variational states. Interestingly, it has been noted that results may depend on the structure of the variational form used. An example is the debated existence of the so-called stripe order, which is a state displaying charge and spin modulations, in the underdoped region of the 2D Hubbard model [22–26]. Other examples concern the proposed spin-liquid character of the Heisenberg antiferromagnet on the kagome lattice [27,28], the variational description of frustrated spin models [29], and Mott insulators [30].

The need for an accurate and easy to prepare variational trial state is transferred in the realm of quantum computation. In the VQE approach, the trial state's ability to describe the desired physical state is determined by the set of gates composing the quantum circuit and is limited by the affordable circuit depth. Because of the limited coherence time of present NISQ machines, it is only possible to run relatively short circuits, with a detrimental impact on the accuracy of the calculation. For example, the unitary coupled cluster *Ansatz* [31], which is the quantum counterpart of the celebrated coupled-cluster technique [32], has been

proposed as a polynomially scaling quantum circuit to solve quantum chemistry problems. However, the number of gates necessary to achieve chemical accuracy, even on small molecules, is simply too large to be successfully executed on NISQ devices [33].

Heuristic circuits, which implement hardware-efficient gates, represent a more realistic approach in the short term, and have been already demonstrated in several small chemical [14,15,34] and lattice model examples [35]. However, they suffer from the same coherence time limitation when investigating larger systems [34].

In this Letter, we introduce a hybrid quantum-classical type of trial states $\mathcal{P}|\psi_c\rangle$, which exploits both the entanglement offered by a short quantum circuit, and projective pseudodynamics, implemented at the classical level, through measurement postprocessing. Here, the projector $\mathcal{P}$ filters out the unwanted high-energy components from the suboptimal trial state $|\psi_c\rangle$, produced by the circuit, and is inspired by established correlated methods, such as variational Monte Carlo calculations [5].

We propose two quite different practical approaches to implement the nonunitary operator $\mathcal{P}$. In the first, the information stored in an ancillary register is used to reweight the measurements performed on the N—qubit circuit register. The second strategy does not require ancillary qubits but the evaluation of the modified Hamiltonian $\mathcal{PHP}$. Depending on the complexity of $\mathcal{P}$, this translates in a polynomial increase of the number of Pauli terms to measure.

Projectors in QMC.—xThe projector $\mathcal{P}$ (partially) removes the residual components of the circuit *Ansatz* $|\psi_c\rangle$ having negligible overlap with the target state (see Supplemental Material [36]). We adopt physically motivated projectors, borrowing inspiration from classical simulations. These are the so-called Jastrow functions, widely used in the QMC community in solving lattice models [37,38] and continuous systems [39], in both first [40–43] and second quantization [44,45].

For example, a particularly simple but effective projector, the so-called Gutzwiller operator [46], counts the number of doubly occupied sites in a lattice, removing such high-energy components in the Hubbard model at large U. The same operator may as well suppress ionic terms naturally arising from a simple single-particle product state description of molecular dissociation.

Jastrow quantum circuit states.—The strategy we propose in this Letter is to act directly on the N-qubit space, e.g., in the case of the Hubbard model, after the Jordan-Wigner mapping of fermionic operator to the qubit space [3,35]. A long-ranged spin Jastrow operator is then applied to the circuit *Ansatz*, using the projector

$$\mathcal{P}_J = e^J, \qquad J = \sum_{k,l=1(k\neq l)}^{N} \lambda_{kl}\sigma_k^z\sigma_l^z, \tag{1}$$

where σ_k^α are Pauli matrices, and $\lambda_{k,l}$ are $N(N-1)/2$ variational parameters. The number of effective optimizable parameters $\boldsymbol{\lambda}$ can be reduced by applying lattice symmetries, for example, by assuming that the value of $\lambda_{k,l}$ only depends on the distance between qubits k and l. The Jastrow correlator can be generalized also to three and more spin interactions. For the sake of brevity, we propose the name *Jastrow quantum circuit* (JQC) for the $\mathcal{P}_J|\psi_c\rangle$ state, reminiscent of the Jastrow-Slater determinant (JSD) wave functions used in electronic QMC calculations [39,47]. In our case the qubit Jastrow operator improves the description of spin correlations by acting on the circuit *Ansatz*, whereas in the classical counterpart it is applied to a mean-field starting state, which imposes the correct (anti) symmetrization of the system. Moreover, it easily includes all possible two qubits k, l interactions being not constrained by the available hardware connectivity [48].

Accuracy of the JQC variational states.—We tested the accuracy of the JQC *Ansatz* on three popular many-body models in one dimension: the transverse field Ising model, $\mathcal{H}_{\text{Ising}} = -\sum_{k,l=0(k\neq l)}^{L-1}\sigma_k^z\sigma_l^z + \Gamma\sum_{k=0}^{L-1}\sigma_k^x$, the Heisenberg model $\mathcal{H}_{\text{Heis}} = -\sum_{k,l=0(k\neq l)}^{L-1}\sigma_k^z\sigma_l^z + \Lambda(\sigma_k^x\sigma_l^x + \sigma_k^y\sigma_l^y)$, and the Hubbard model $\mathcal{H}_{\text{Hub}} = -t\sum_{k=0}^{L-1}\sum_{s=\uparrow,\downarrow}(c_{k,s}^\dagger c_{k+1,s} + c_{k+1,s}^\dagger c_{k,s}) + U\sum_{k=0}^{L-1}(c_{k,\uparrow}^\dagger c_{k,\uparrow}c_{k,\downarrow}^\dagger c_{k,\downarrow})$ at half-filling, where $c_{k,s}^\dagger$ ($c_{k,s}$) are fermionic creation (destruction) operators at site i, and t, U are the hopping and on-site Coulomb repulsion parameters, respectively. While the first two models do not require any mapping, being already spin Hamiltonians (therefore $N = L$), we use the mapping between spinful electrons and qubits, illustrated in Refs. [38,49], to map a L-site Hubbard model into a $N = 2L$ qubit register with ladder connectivity (see also Supplemental Material [36]).

In this Letter we use a primitive heuristic R_y-CNOT circuit. The circuit *Ansatz* is represented by $|\psi_c(\boldsymbol{\theta})\rangle = U_c(\boldsymbol{\theta})|\psi_{\text{init}}\rangle$, where $U_c(\boldsymbol{\theta})$ is the unitary operator representing the circuit, $\boldsymbol{\theta}$ is the set of total $d\,N$ single-qubit rotation angles, where d is the circuit depth, and $|\psi_{\text{init}}\rangle$ is an easy-to-prepare bit string. While such type of circuit requires an affordable number of entangling gates (CNOT) per block, it may not respect basic symmetries of the desired solution, compatible with the particle and spin number conservation [34].

In this case, the nonunitary Jastrow operator will effectively project out wave-function components of $|\psi_c\rangle$ having particle number and magnetization incompatible with the Heisenberg and Hubbard models. While the Jastrow operator cannot recover the exact energy by itself, irrespectively of the circuit, it uniformly improves the standard VQE *Ansatz* $|\psi_c(\boldsymbol{\theta})\rangle$, for all the three models considered. In fact, as we observe a several order-of-magnitude improvement of the energy at fixed circuit depths (see Fig 1). As discussed above, the total number of variational parameters in the set $(\boldsymbol{\theta}, \boldsymbol{\lambda})$ is linearly increasing with N, if appropriate lattice symmetries

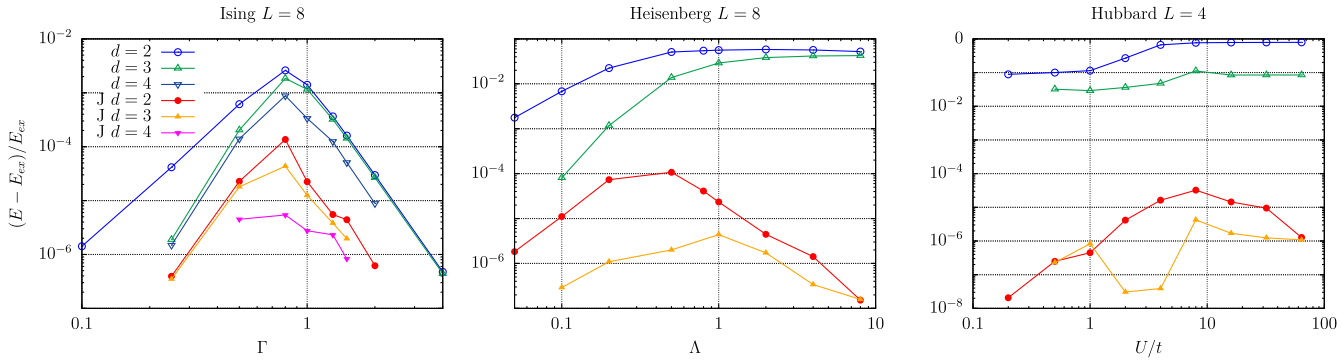

FIG. 1. Accuracy of the JQC state for one-dimensional many-body problems. Relative energy differences are shown as a function of the relevant Ising, Heisenberg, and Hubbard model parameters. Energies computed for selected circuit depths d are plotted for the circuit *Ansatz* (empty symbols, blue and green) and for the JQC (solid, red, and orange). All system sizes translate into a $N = 8$ qubit register. While the JQC *Ansatz* always improves upon the circuit one, notably the worst performance is around the critical points of the models, i.e., when Γ, Λ, $U/4t = 1$, respectively. The number of Jastrow optimizable variational parameters, exploiting lattice symmetries, is 7 in the case of Ising and Heisenberg models, and 10 for Hubbard (see Supplemental Material [36]). For each setup we plot the best outcome among several repetitions of the numerical optimization procedure.

are taken into account [36], or if a cutoff is imposed on the correlation lengths considered in Eq. (1). While in Fig. 1 we benchmark the quality of the *Ansatz* at fixed system sizes by varying the model parameters, in the Supplemental Material we investigate the efficiency of our method as a function of the system size [36]. These results have been obtained simulating the circuit in noiseless conditions and applying exactly the Jastrow operator on the state vector $|\psi_c\rangle$. Since the JQC state is not normalized to unity, the normalization has been computed numerically.

Implementation 1: Using entangled copies.—Differently to classical simulations, implementing the projector is not as straightforward. In this section we will illustrate the general procedure, while developing in parallel an example (a $L = 2$ sites Ising model). The standard VQE approach would require a 2-qubit circuit, and measuring expectation values of the ZZ, XI, and IX operators, to calculate the energy of the model [14]. In practical approaches (as implemented in the QISKIT package [50]) this is done partitioning the Hamiltonian in groups of operators that can be measured simultaneously $H = \sum_{\mathbf{b}} H_{\mathbf{b}}$, in a given basis $\mathbf{b}$. The expectation value $\langle H_{\mathbf{b}} \rangle$ is evaluated by reconstructing the bit-string probability $P_{\mathbf{b}}(i)$ in the $\mathbf{b}$ basis, through measurements (here the label i denotes the integer encoded in the L-bit string) [51]. Suitable unitaries (called postrotations $\mathcal{R}_\alpha$) allows us to measure in different bases. In this example, to measure the nondiagonal operator we need $\mathcal{R}_\alpha = H$, where H is the Hadamard matrix.

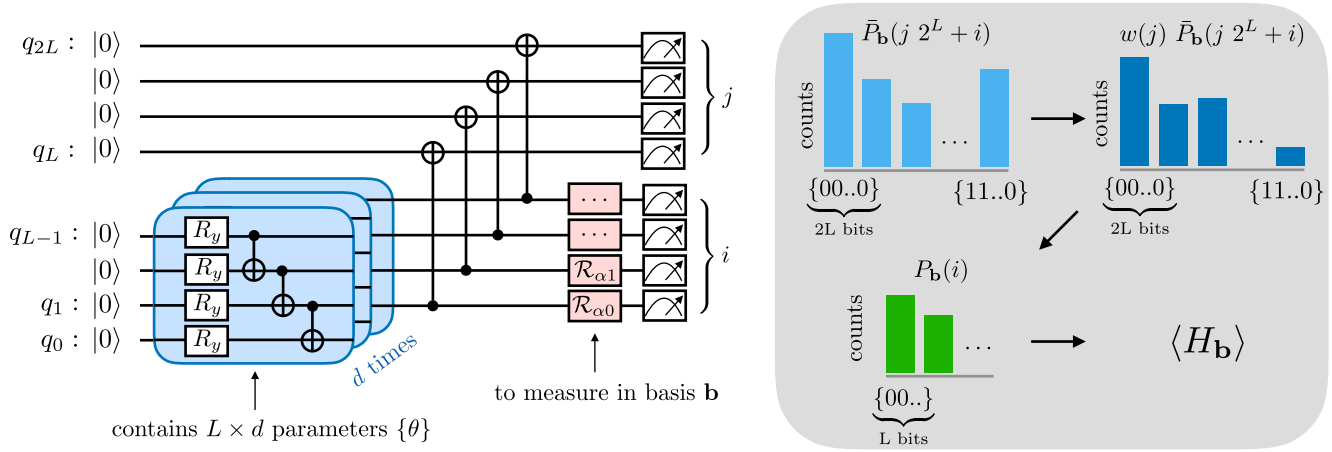

FIG. 2. Hardware implementation and classical postprocessing. (Left) Circuit realizing the entangled copy of the state produced by the variational block (blue). The most tested variational form in this work is the R_y CNOT, made by d repetitions of blocks. Each of them features L parametrized single qubits rotations R_y, and a cascade of L-1 CNOT gates. Postrotations are applied only on L qubits to measure outcomes in a given basis $\mathbf{b}$. (Right) For each basis $\mathbf{b}$, the normalized measured count $\bar{P}_{\mathbf{b}}$ of the $2L$-bit possible outcomes (each of them univocally defined by the integer $2^L j + i$), is reweighted according to the Jastrow function. The probability distribution $P_{\mathbf{b}}$, defined on L-bit strings, is then recovered and used to evaluate the expectation value of H_b (see main text).

In our approach, we need to combine the possibility of measuring the qubits after applying the postrotations, with the requirements to also read the qubits in their Z basis, to evaluate Eq. (1). This is possible only by introducing an ancillary register of the same size L. We use the ancilla register to store an entangled copy of the original register, using CNOT gates as in Fig. 2. In this specific case, the total register now reads $\{q_0, q_1.q_2, q_3\}$, where the first $L = 2$ qubits evolve through the circuit, and the last ones are initialized to 0. The L-bit outcome j of the ancilla register measurement determines a weight $w(j)$, to be applied to the $2L$-bit readout, labeled with the integer $2^L j + i$. The only additional step required is to reconstruct the reduced probability of the original 2-bits components $P_{\rm b}(i)$, given the total probability of the 4-bits strings $\bar{P}_{\rm b}(2^L j + i)$, which is actually measured and then reweighted (see Supplemental Material [36]).

In Fig. 3 we benchmark the proposed reweighting scheme on synthetic measurements (i.e., using circuit simulators, with and without noise), and real datasets from IBM Q hardware, Tokyo and Tenerife, using $L = 2$ and $L = 4$ Ising models, and with two different circuit *Ansätze*.

The first circuit is made of two Hadamard gates, $U_c = H \otimes H$, that produces an equal superposition state Here, it can be shown analytically that a two-spin Jastrow operator [see Eq. (1)] suffices to amplify (suppress) the components having even (odd) parity, recovering the (unnormalized) exact state, for $\lambda = \lambda_{01} \approx 0.24$ [52].

The obtained energies from the circuit simulations and the Tokyo machine data are compatible with the predicted values at various λ, obtained by state-vector emulations of the process. We observe that for the Tenerife hardware data the one-parameter Jastrow operator is not sufficient to recover the exact energy of the model, because of the noise level of the hardware. Nevertheless, the Jastrow operator allows us to improve the circuit energy, although for a different value of λ compared to the theoretically predicted one.

The technique is also demonstrated on a more challenging $L = 4$ system (which translates into a $2L = 8$-qubit register). Here, the Jastrow projector recovers the energy difference between a heuristic R_y-CNOT (with $d = 1$ and optimized $\boldsymbol{\theta}$ parameters) energy E_c and the exact one.

Implementation 2: Measuring a transformed Hamiltonian.—The second implementation we propose requires additional Pauli operators to be measured, instead of ancilla qubits. Computing the expectation value of the energy on the JQC state $E = \langle \mathcal{P}_J \psi_c | \mathcal{H} | \mathcal{P}_J \psi_c \rangle / \langle \mathcal{P}_J \psi_c | \mathcal{P}_J \psi_c \rangle$, it is equivalent to measure the ratio of $\mathcal{P}_J \mathcal{H} \mathcal{P}_J$ and $\mathcal{P}_J \mathcal{P}_J$ operators on ψ_c. Unfortunately, we notice that Eq. (1) results in an exponentially increasing number of Pauli operators with the register size. However, a suitably truncated expansion $\mathcal{P}'_J = 1 + J + J^2/2 + \cdots$, controlled by the smallness of the parameters $\boldsymbol{\lambda}$, can still be effective while reducing the number of operators to polynomial scaling (we report numerical benchmarks in the Supplemental Material [36]).

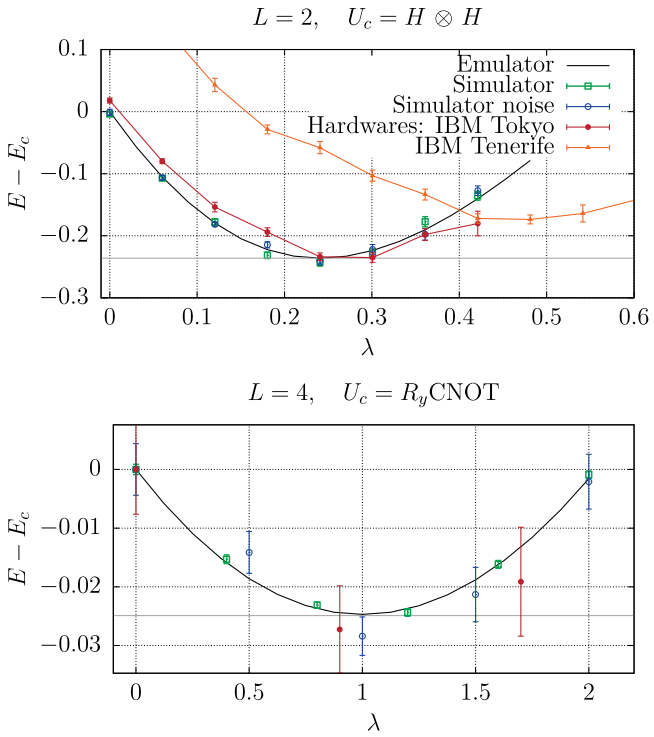

FIG. 3. JQC *Ansatz* on hardware and circuit simulators. (Top panel) Energy difference of the JQC states compared to the circuit energy E_c for a $L = 2$ Ising model as a function of the single Jastrow parameter λ (see main text). The circuit considered is $U_c = H \otimes H$. The black (gray) line represents the exact energy of the JQC *Ansatz* (of the Ising model). Colored points are obtained implementing the extended circuit of Fig. 2 with simulators (green, noiseless simulator; blue, noise model from IBM Tokyo chip) and with hardware (red, IBM Tokyo chip; orange, IBM Tenerife), and using the measurements reweighting method introduced in the main text. For each λ point we reconstruct $\bar{P}_{\mathbf{b}}$, for the two basis, using 8192 shots. Error bars are computed repeating this process $M_{\rm rep} = 12$ times. The JQC state reduces to ψ_c for $\lambda = 0$. (Bottom panel) Same analysis as above, but on a $L = 4$ system and using an entangled R_yCNOT circuit. Here, the Jastrow operator contains three variational parameters, this set $\lambda_{\rm opt}$ is optimized beforehand. In order to have a one-dimensional plot we multiply them elementwise by λ, such that when $\lambda = 1$ we reobtain the optimal solution. In the noiseless simulator case we acquire 2×10^6 shots, with $M_{\rm rep} = 24$. In the noisy simulator (hardware) case we acquire 1.6×10^5 (2.5×10^4) shots, and $M_{\rm rep} = 12(24)$. In the latter cases, a rigid shift of ≈ 0.15 is applied to the data series so that the $\lambda = 0$ point is at $E - E_c = 0$.

Conclusions.—We introduce hybrid quantum-classical states to solve many-body lattice models, drastically reducing the depth requirements of the heuristic circuits to reach target accuracy, by leveraging on the use of nonunitary operators [53]. The approach is variational, and after full optimization of the Jastrow parameters the energy is always better or—in the worst case—equal to the one provided by the circuit *Ansatz*. Two practical schemes

have been proposed to realize such states in the present hardware. The most promising one requires an additional ancillary register. This method relies on measurement reweighting and allows for an exact implementation of the Jastrow correlation operator, while it does not increase the number of Pauli operators to be measured, that already constitutes a drawback of standard VQE [12]. The approach has been demonstrated using an 8-qubit circuit in the IBM Tokyo chip, providing quantitative energetics for the test case Ising model. We notice that this implementation extends the scope of the recently proposed stabilizer-VQE method [54], where measurements are simply discarded using an error detection scheme. In this case, the projector allows us to improve the accuracy of the VQE *Ansatz*, while also mitigating the possible errors. A possible issue of these approaches may arise when the VQE *Ansatz* and the exact state have negligible overlap. In our case, an increased statistical fluctuation of the energy would be a fingerprint that most of the measurements are reweighted to zero. While this issue is not present in the studied cases (see Supplemental Material [36]), it will call for the development of synergic circuit and projector operators. We anticipate the use of suitably modified projected circuit states for solving quantum chemistry problems.

We acknowledge discussions with L. Guidoni, F. Benfenati, N. Moll, and S. Sorella. The authors acknowledge financial support from the Swiss National Science Foundation (SNSF) through Grant No. 200021-179312.

*GMA@zurich.ibm.com

[1] R. P. Feynman, Simulating physics with computers, Int. J. Theor. Phys. **21**, 467 (1982).
[2] B. P. Lanyon, J. D. Whitfield, G. G. Gillett, M. E. Goggin, M. P. Almeida, I. Kassal, J. D. Biamonte, M. Mohseni, B. J. Powell, M. Barbieri, *et al.*, Towards quantum chemistry on a quantum computer, Nat. Chem. **2**, 106 (2010).
[3] D. Wecker, M. B. Hastings, N. Wiebe, B. K. Clark, C. Nayak, and M. Troyer, Solving strongly correlated electron models on a quantum computer, Phys. Rev. A **92**, 062318 (2015).
[4] M. Troyer and U.-J. Wiese, Computational Complexity and Fundamental Limitations to Fermionic Quantum Monte Carlo Simulations, Phys. Rev. Lett. **94**, 170201 (2005).
[5] F. Becca and S. Sorella, *Quantum Monte Carlo Approaches for Correlated Systems*, 1st ed. (Cambridge University Press, Cambridge, England, 2017).
[6] J. Preskill, Quantum computing in the NISQ era, and beyond, Quantum **2**, 79 (2018).
[7] N. Moll, P. Barkoutsos, L. S. Bishop, J. M. Chow, A. Cross, D. J. Egger, S. Filipp, A. Fuhrer, J. M. Gambetta, M. Ganzhorn, A. Kandala, A. Mezzacapo, P. Müller, W. Riess, G. Salis, J. Smolin, I. Tavernelli, and K. Temme, Quantum optimization using variational algorithms on near-term quantum devices, Quantum Sci. Technol. **3**, 030503 (2018).
[8] A. Cross, L. Bishop, S. Sheldon, P. D. Nation, and J. M. Gambetta, Validating quantum computers using randomized model circuits, arXiv:1811.12926.
[9] A. Peruzzo, J. McClean, P. Shadbolt, M.-H. Yung, X.-Q. Zhou, P. J. Love, A. Aspuru-Guzik, and J. L. Obrien, A variational eigenvalue solver on a photonic quantum processor, Nat. Commun. **5**, 4213 (2014).
[10] I. D. Kivlichan, J. McClean, N. Wiebe, C. Gidney, A. Aspuru-Guzik, G. K.-L. Chan, and R. Babbush, Quantum Simulation of Electronic Structure with Linear Depth and Connectivity, Phys. Rev. Lett. **120**, 110501 (2018).
[11] Y. Shen, X. Zhang, S. Zhang, J. Zhang, M. Yung, and K. Kim, Quantum implementation of the unitary coupled cluster for simulating molecular electronic structure, Phys. Rev. A **95**, 020501(R) (2017).
[12] D. Wecker, M. B. Hastings, and M. Troyer, Progress towards practical quantum variational algorithms, Phys. Rev. A **92**, 042303 (2015).
[13] P. O'Malley *et al.*, Scalable Quantum Simulation of Molecular Energies, Phys. Rev. X **6**, 031007 (2016).
[14] A. Kandala, A. Mezzacapo, K. Temme, M. Takita, M. Brink, J. M. Chow, and J. M. Gambetta, Hardware-efficient variational quantum eigensolver for small molecules and quantum magnets, Nature (London) **549**, 242 (2017).
[15] M. Ganzhorn, D. J. Egger, P. K. Barkoutsos, P. Ollitrault, G. Salis, N. Moll, A. Fuhrer, P. Mueller, S. Woerner, I. Tavernelli, and S. Filipp, Gate-Efficient Simulation of Molecular Eigenstates on a Quantum Computer, Phys. Rev. Applied **11**, 044092 (2019).
[16] C. Hempel, C. Maier, J. Romero, J. McClean, T. Monz, H. Shen, P. Jurcevic, B. P. Lanyon, P. Love, R. Babbush, A. Aspuru-Guzik, R. Blatt, and C. F. Roos, Quantum Chemistry Calculations on a Trapped-Ion Quantum Simulator, Phys. Rev. X **8**, 031022 (2018).
[17] M. Schwarz, K. Temme, and F. Verstraete, Preparing Projected Entangled Pair States on a Quantum Computer, Phys. Rev. Lett. **108**, 110502 (2012).
[18] E.g., the generation of the Hamiltonian parameters that always require a classical preprocessing tool.
[19] E. Dagotto, Correlated electrons in high-temperature superconductors, Rev. Mod. Phys. **66**, 763 (1994).
[20] E. Dagotto, Complexity in strongly correlated electronic systems, Science **309**, 257 (2005).
[21] J. P. F. LeBlanc *et al.*, Solutions of the Two-Dimensional Hubbard Model: Benchmarks and Results from a Wide Range of Numerical Algorithms, Phys. Rev. X **5**, 041041 (2015).
[22] B.-X. Zheng, C.-M. Chung, P. Corboz, G. Ehlers, M.-P. Qin, R. M. Noack, H. Shi, S. R. White, S. Zhang, and G. K.-L. Chan, Stripe order in the underdoped region of the two-dimensional Hubbard model, Science **358**, 1155 (2017).
[23] P. Corboz, T. M. Rice, and M. Troyer, Competing States in the *t-j* Model: Uniform *d*-Wave State Versus Stripe State, Phys. Rev. Lett. **113**, 046402 (2014).
[24] S. Sorella, G. B. Martins, F. Becca, C. Gazza, L. Capriotti, A. Parola, and E. Dagotto, Superconductivity in the Two-Dimensional *t-J* Model, Phys. Rev. Lett. **88**, 117002 (2002).
[25] W.-J. Hu, F. Becca, and S. Sorella, Absence of static stripes in the two-dimensional *t-j* model determined using an

accurate and systematic quantum Monte Carlo approach, Phys. Rev. B **85**, 081110(R) (2012).

[26] In this case, correlated mean-field approximations suggest a uniform *d*-wave superconducting solution, while density matrix renormalization group states may be biased toward a stripe ordering.

[27] H.-C. Jiang, Z. Wang, and L. Balents, Identifying topological order by entanglement entropy, Nat. Phys. **8**, 902 (2012).

[28] Y. Iqbal, F. Becca, S. Sorella, and D. Poilblanc, Gapless spin-liquid phase in the kagome spin-$\frac{1}{2}$ Heisenberg antiferromagnet, Phys. Rev. B **87**, 060405(R) (2013).

[29] L. Capriotti, F. Becca, A. Parola, and S. Sorella, Resonating Valence Bond Wave Functions for Strongly Frustrated Spin Systems, Phys. Rev. Lett. **87**, 097201 (2001).

[30] M. Capello, F. Becca, M. Fabrizio, S. Sorella, and E. Tosatti, Variational Description of Mott Insulators, Phys. Rev. Lett. **94**, 026406 (2005).

[31] J. D. Watts, G. W. Trucks, and R. J. Bartlett, Coupled-cluster, unitary coupled-cluster and MBTP(4) open-shell analytical gradient methods, Chem. Phys. Lett. **164**, 502 (1989).

[32] R. J. Bartlett and G. D. Purvis, Many-body perturbation theory, coupled-pair many-electron theory, and the importance of quadruple excitations for the correlation problem, Int. J. Quantum Chem. **14**, 561 (1978).

[33] D. Wecker, B. Bauer, B. K. Clark, M. B. Hastings, and M. Troyer, Gate-count estimates for performing quantum chemistry on small quantum computers, Phys. Rev. A **90**, 022305 (2014).

[34] P. K. Barkoutsos, J. F. Gonthier, I. Sokolov, N. Moll, G. Salis, A. Fuhrer, M. Ganzhorn, D. J. Egger, M. Troyer, A. Mezzacapo, S. Filipp, and I. Tavernelli, Quantum algorithms for electronic structure calculations: Particle-hole Hamiltonian and optimized wave-function expansions, Phys. Rev. A **98**, 022322 (2018).

[35] J.-M. Reiner, M. Marthaler, J. Braumüller, M. Weides, and G. Schön, Emulating the one-dimensional Fermi-Hubbard model by a double chain of qubits, Phys. Rev. A **94**, 032338 (2016).

[36] See Supplemental Material at http://link.aps.org/supplemental/10.1103/PhysRevLett.123.130501 for more details concerning the procedure, the quantum circuit for the Hubbard models, additional results, and benchmarks.

[37] E. Manousakis, The spin-1/2 Heisenberg antiferromagnet on a square lattice and its application to the cuprous oxides, Rev. Mod. Phys. **63**, 1 (1991).

[38] L. Spanu, M. Lugas, F. Becca, and S. Sorella, Magnetism and superconductivity in the t-t'-j model, Phys. Rev. B **77** (2008) 024510.

[39] R. Jastrow, Many-body problem with strong forces, Phys. Rev. **98**, 1479 (1955).

[40] M. Casula, C. Attaccalite, and S. Sorella, Correlated geminal wave function for molecules: An efficient resonating valence bond approach, J. Chem. Phys. **121**, 7110 (2004).

[41] A. Zen, E. Coccia, Y. Luo, S. Sorella, and L. Guidoni, Static and dynamical correlation in diradical molecules by quantum Monte Carlo using the Jastrow antisymmetrized geminal power ansatz, J. Chem. Theory Comput. **10**, 1048 (2014).

[42] G. Mazzola, R. Helled, and S. Sorella, Phase Diagram of Hydrogen and a Hydrogen-Helium Mixture at Planetary Conditions by Quantum Monte Carlo Simulations, Phys. Rev. Lett. **120**, 025701 (2018).

[43] C. Genovese, A. Meninno, and S. Sorella, Assessing the accuracy of the Jastrow antisymmetrized geminal power in the H_4 model system, J. Chem. Phys. **150**, 084102 (2019).

[44] E. Neuscamman, The Jastrow antisymmetric geminal power in Hilbert space: Theory, benchmarking, and application to a novel transition state, J. Chem. Phys. **139**, 194105 (2013).

[45] E. Neuscamman, Communication: A Jastrow factor coupled cluster theory for weak and strong electron correlation, J. Chem. Phys. **139**, 181101 (2013).

[46] M. C. Gutzwiller, Effect of Correlation on the Ferromagnetism of Transition Metals, Phys. Rev. Lett. **10**, 159 (1963).

[47] W. M. C. Foulkes, L. Mitas, R. J. Needs, and G. Rajagopal, Quantum Monte Carlo simulations of solids, Rev. Mod. Phys. **73**, 33 (2001).

[48] I. D. Kivlichan, J. McClean, N. Wiebe, C. Gidney, A. Aspuru-Guzik, G. K.-L. Chan, and R. Babbush, Quantum Simulation of Electronic Structure with Linear Depth and Connectivity, Phys. Rev. Lett. **120**, 110501 (2018).

[49] F. Verstraete and J. I. Cirac, Mapping local Hamiltonians of fermions to local Hamiltonians of spins, J. Stat. Mech. (2005) P09012.

[50] G. Aleksandrowicz *et al.*, QISKit open source quantum information software kit, https://www.qiskit.org/.

[51] For example, we have $\langle XI + IX\rangle = -2x_{00} + 0x_{10} + 0x_{01} + 2x_{11}$,where x_i is the normalized count of the 2-bit string readout i in basis $\{X, X\}$.

[52] Notice also that in this limiting case the circuit state is a trivial product state, and the Jastrow operator recovers all the missing correlations characterizing the exact state.

[53] M. Motta, C. Sun, A. T. K. Tan, M. J. Rourke, E. Ye, A. J. Minnich, F. G. Brandao, and G. K. Chan, Quantum imaginary time evolution, quantum Lanczos, and quantum thermal averaging, arXiv:1901.07653.

[54] S. McArdle, X. Yuan, and S. Benjamin, Error-Mitigated Digital Quantum Simulation, Phys. Rev. Lett. **122**, 180501 (2019).